Hindawi
International Transactions on Electrical Energy Systems
Volume 2022, Article ID 8004425, 13 pages
https://doi.org/10.1155/2022/8004425

Research Article

Elimination of Harmonics in Multilevel Inverter Using Multi-Group Marine Predator Algorithm-Based Enhanced RNN

G. Krithiga and V. Mohan

Department of Electrical and Electronics Engineering, E.G.S. Pillay Engineering College, Nagapattinam, Tamilnadu, India

Correspondence should be addressed to G. Krithiga; krithiga.g2012@gmail.com

Received 23 March 2022; Revised 12 May 2022; Accepted 24 May 2022; Published 29 June 2022

Academic Editor: R Sitharthan

Multilevel inverters (MLI) are becoming more common in different power applications, such as active filters, elective vehicle drives, and dc power sources. The Multi-Group Marine Predator Algorithm (MGMPA) is introduced in this study for resolving transcendental nonlinear equations utilizing an MLI in a selective harmonic elimination (SHE) approach. Its applicability and superiority over various SHE approaches utilized in recent research may be attributed to its high accuracy, high likelihood of convergence, and improved output voltage quality. For the entire modulation index, the optimum switching angles (SA) from Marine Predator Algorithm (MPA) is utilized to control a three-phase 11-level MLI employing cascaded H-bridge (CHB) architecture to regulate the vital element and eliminate the harmonics. The limitation of SHE is that it is difficult to find solutions for nonlinear equations. As a result, specific optimization approaches must be used. Artificial Intelligence (AI) algorithms can handle such a nonlinear transcendental equation successfully, although their time consumption as well as convergence abilities vary. Here, recurrent neural network (RNN) is considered where the hidden neurons are tuned by MGMPA with the intention of harmonic distortion parameter (HDP) minimization, thus called as enhanced recurrent neural network (ERNN). The method's resilience and consistency are demonstrated by simulation and analytical findings. The MGMPA method is more effective and appropriate than various algorithms including the MPA, Harris Hawks optimization (HHO), and Whale optimization algorithm (WOA), according to simulation data.

1. Introduction

The demand for electrical energy is growing every day. As a result, conventional energy sources are becoming depleted. A lot of research has gone into getting power from renewable energy sources. Regardless of environmental considerations, all power electronics and power system research societies have picked solar and wind energy as the most popular renewable energy sources. Power converter technologies that can control and manage power are required for obtaining maximum power and improving the quality of power obtained from renewable energy sources. The loads usually require ac electricity to operate [1]. As a result, it is evident that an inverter is the most crucial component of a renewable energy power conversion system.

Since 1975, the multilevel inverter (MLI) has been used as an alternative in high-power and medium-voltage applications. MLI research has gotten a lot of attention in the last three decades since it offers a lot of advantages over the typical two-level inverter with pulse-width modulation (PWM). The output voltage generated by the inverters will be increased when the numbers of levels increase. The output waveform will be in the shape of staircase making a considerable reduction in harmonics [2].

PWM management for power converters has been studied and used in industrial applications [3]. PWM approaches were recommended over high-frequency PWM approaches for medium-voltage and high-power applications. Selective harmonic elimination (SHE) produced a higher quality waveform at a reduced frequency [4, 5]. The fundamental challenge in using SHEPWM was getting

switching angles by resolving nonlinear transcendental equations. Numerical approaches, optimization approaches, and algebraic methodologies have all been offered for the switching angle computation. Yet, in the use of SHEPWM, calculating switching angles remains a difficult job. In the previous, PWM approaches for the effective functioning of power electronics converters have been widely explored and deployed [6]. It delivers the required vital element at the output with the least amount of unwanted harmonics. Nevertheless, high-sinusoidal PWM (SPWM) approaches like carrier-based modulation and space vector-based PWM (SVPWM) received the most attention. A high-frequency carrier was continually contrasted with a basic element (preferred component) in SPWM, and pulses were created at intersection sites. The unique switching states are initially detected in SVPWM, and then these vectors are employed to get the required output [7]. The key benefit is that they allow you to have the required output parts while also moving the harmonics component to the sub-band at the switching frequency, resulting in less filtering [8]. Two-level voltage-source inverters (VSIs) were often utilized in the past, and several PWM algorithms for two-level VSI were devised [9]. Higher power processing requirements, on the other hand, open up the possibility of developing novel converter architectures to handle rising power needs while working with constrained current ratings and semiconductor device voltage.

Nowadays, the main multilevel configurations have been studied and recommended, including cascaded H-bridge (CHB), neutral point clamped (NPC), flying capacitor (FC), active NPC (ANPC), modular multilevel converter (MMC), and numerous reduced device count emerging subnetworks [10]. Good quality output waveforms (Stepped) and therefore reduced total harmonic distortion (THD), lower inventive switching frequency, utilization of current rating semiconductor switches and low voltage, and creation of tiny dv/dt at switches are all critical elements of these architectures [11]. For the management and operation of these MLI topologies, high switching frequency-oriented PWM approaches are favored because the output waveform level is improved according to IEEE 591 standards. Nevertheless, switching losses must be addressed in high-power multilayer converter applications, which has a significant impact on effectiveness [12]. Low switching frequency-oriented PWM approaches like SHE, selective harmonics mitigation (SHM), optimum PWM (OPWM) approaches, synchronous optimum PWM (SOPWM), THD minimization PWM approaches, and pulse-width amplitude modulation are discussed in this perspective [13]. These approaches are known as preprogrammed PWM approaches because they are tuned to meet certain needs, like removing certain harmonics, reducing certain harmonics to a given level, and managing total harmonic content in the output waveform [14]. Lower order harmonics are evaluated for full removal in SHEPWM, while the requisite real part is maintained concurrently [15]. The count of switching angles taken into account in quarter-wave determines how many harmonics may be removed [16]. Additional harmonics are removed as the count of switching angles (SA) is increased at the cost of increasing losses. As a result, the output power quality and switching loss must be balanced [17]. As a modulation index function, the SHE equations, determined by Fourier series, present three alternatives: a single solution, numerous solutions, and no solution [18]. Distinct THD and non-eliminated harmonics result from numerous solutions in few modulation index ranges. As a result, the entire solutions from the resulting system must be found [19].

Various approaches have been developed in the literature throughout the years to handle the system of simultaneous SHE equations [20]. Mathematical approaches-oriented iterative techniques, meta-heuristic-oriented optimizes techniques, and algebraic approaches are the three types [21]. Numerical-oriented iterative approaches are quickly convergent, and solutions may be produced with the appropriate precision. The key obstacle in using these strategies, though, is selecting appropriate initial assumptions and computing derivatives in each iteration, which leads to singularity difficulties and solution divergence [22]. An objective is addressed with varying restrictions on the harmonic frequencies in meta-heuristic approaches. Glover [23] coined the term "meta-heuristics," which refers to a group of potential methods for solving difficult optimization issues. The meta-heuristic algorithms try to identify near-optimal solutions by exploring the search space efficiently and comprehensively utilising governing mechanisms that emulate particular methods borrowed from nature, social behaviour, physical laws, and so on. Particle swarm optimization (PSO), modified PSO, genetic algorithm (GA), differential evolution (DE), ant colony optimization (ACO), artificial bee colony (ABC), teaching learning (TL), hybrid PSO and GA, grey wolf optimization (GWO), Flower pollination algorithm (FPA), and other modern approaches are used to optimize the objective function [24]. Slow convergence, initial guess, accurate selection, and greater computing time are the key challenges when using a meta-heuristic-oriented optimization approach. The SHE equations are converted into algebraic equations utilizing trigonometric formulae and then resolved employing the Walsh technique, symmetric polynomial techniques, and Groebner bases in algebraic techniques [4]. All of the solutions to the SHE equation may be found using algebraic techniques, with precise values. Nevertheless, when the count of switching angles grows, the polynomial degree grows exponentially; hence these techniques are only utilized to compute a few SAs [25] which discuss capacitor voltage utilizing SHEPWM for systems. Artificial neural network (ANN), Hopfield NNs, data fitting, and other techniques have been used to effectively execute the real-world application of SHEPWM. The switching angles are calculated initially using any of the methods outlined above, and then implemented in real time for diverse purposes.

The paper contribution is as follows:

(i) to introduce Multi-Group Marine Predator Algorithm (MGMPA) for resolving transcendental nonlinear equations utilizing an MLI in a SHE approach;

(ii) to utilize the optimum SAs from Marine Predator Algorithm (MPA) to control a three-phase 11-level MLI employing CHB architecture to regulate the vital element and eliminate the low order harmonics;

(iii) to develop enhanced recurrent neural network (ERNN), where the hidden neurons of recurrent neural network (RNN) are tuned by MGMPA with the intention of harmonic distortion parameter (HDP) minimization;

(iv) to demonstrate the method's resilience and consistency by simulation and analytical findings.

The paper organization is as follows. Section 1 is the introduction of MLI. The literature works of MLI are in Section 2. Section 3 explains the MLI for the harmonics elimination. The THD and SHEPWM techniques in MLI are explained in Section 4. Section 5 describes the ERNN and MGMPA for the MLI. The results are in Section 6. Section 7 is conclusion.

2. Literature Survey

2.1. Related Works. In 2021, Ahmad et al. [26] have introduced a new rapid convergent homotopy perturbation method (HPM) for computing multilevel inverter switching angles at a quicker pace. The suggested strategy produced answers that are as precise as algebraic techniques but do not rely on the initial estimate. In certain modulation index ranges, the suggested approach can calculate a bigger count of switching angles having various solutions. To confirm the outcomes for actual applications, a prototype was created and the calculated switching angles were validated utilizing a field-programmable gate array (FPGA) controller.

In 2019, Kim and Lee [27] have suggested a PWM system that combines two modulation techniques. Furthermore, to equally divide power and shape currents having minimal loss, an extra cell rotation approach is presented. The simulation findings supported the suggested modulation system's validity.

In 2021, Barbie et al. [28] have developed and utilized a unique live-voltage weighted THD (WLTHD) with the goal of decreasing THD. The suggested WLTHD describes a function of complete conceivable PSA, and was applicable to any MLI with N values, odd or even. Furthermore, the current WLTHD reduction strategy was demonstrated to be a special instance of the recommended generic method. The resulting approach, which was capable of producing technically correct symbolic WLTHD findings, was compared to quantitatively attained outcomes in prior studies. Validation using the controller + hardware-in-loop (C-HIL) technique for seven-level three-phase MLIs for present optimization is also performed, indicating considerable gains over earlier achieved techniques. Even for highly resistive loads, the suggested WLTHD reduction has the strongest correlation to present. For the benefit of the reader, links to download Maple and MATLAB of suggested WLTHD, and premeasured optimal phase switching angle (PSA) values for 5°N 16, which covered practical situations, were also supplied.

In 2021, Buccella et al. [29] have proposed CHB using changeable dc sources. A theoretical argument was offered for a certain count of switching angles, which represents the count of dc sources. The dc voltage sources fluctuated linearly as per the approach, but the SAs were unaffected. The overall harmonic distortion of the resultant output voltage was minimal, and it was independent. The suggested process lowered distortion across a wider range of modulation indexes when compared to a standard selective harmonic removal approach as well as a pulse amplitude technique.

In 2020, Gunasekaran and Karthikeyan [30] by attempting to implement nonlinear transformational optimization (NTO) method have suggested an advancement process to register SAs, akin to reducing voltage harmonics, time, control over the large extend of multilevel inverters (MLI) is knowledgeable. The suggested approach was performed to the point where each conceivable course of action was obtained without first doing a proper evaluation at the resolves. Furthermore, this strategy was appropriate for higher order MLI, where various traditional techniques were unable to handle the switching angles owing to a higher computing burden. The arrangements that carried the least THD in the output voltage were produced for the estimates of regulation records in which several solutions exist. Try additional arrangement groups instead of picking a single group of solutions to get a significant reduction in THD. An eleven-level CHB inverter-oriented method was used to corroborate the simulation outcomes. As a result, both exploratory and simulation results suggested that our methodology outperformed the commonly used phase-voltage THD reduction method.

An adaptive neuro-fuzzy interference system (ANFIS) was installed in the multilayer inverter to eliminate voltage harmonics [31]. It was accomplished by lowering the THD of the MLI. From the reference voltage, the voltage changes of the multilayer inverter were calculated. The ANFIS has been subjected to voltage variations at various time intervals. The switching angles could be created by the interference system based on voltage fluctuations. These switching angles might result in a lower THD multilayer inverter output voltage. The suggested process was analyzed in the MATLAB/Simulink development environment. The efficacy of the suggested technique was assessed using the output voltage of an MLI without a controller and with a neuro-fuzzy controller (NFC).

An MLI for photovoltaic system has been conceived and executed [32]. The MLI in the developed framework employed PWM to transform DC electricity. The efficiency of reducing voltage was investigated in the PWM approach and contrasted to the SPWM technique. ANFIS was also used in this study to estimate the optimum switch angles and modulation index for a five-level CHB having increased voltage. The Newton Raphson (NR) approach was used to gather the data group for the ANFIS-oriented study. With any random beginning estimate and any count of levels of an MLI, the suggested prediction technique was more compelling than existing approaches in offering the entire feasible solutions. The simulation outcomes showed that

utilizing the best switching angles and modulation index, lower-order harmonics were removed. To show the efficacy of the suggested system, a prototype system was developed.

In 2016, Sudha et al. [33] in a solar-powered CHBMLI have presented an innovative way to remove harmonics. To solve the problems and achieve the best SAs, the issue employed NR and PSO-oriented SHE approaches. The optimal switching angles were determined in offline mode and it is used for reducing the THD. The solution related to the nonlinear transcendental equations was a fundamental consideration. Nevertheless, utilizing the ANFIS/constant voltage maximum power point tracker (MPPT) algorithm, the suggested technique might tackle this conflict in a simplified manner by simply transforming nonequal into equal dc sources. The performance of a PV-fed 11-level CHBMLI with induction motor driving was assessed using simulated data. An experimental version of CHBMLI was used to confirm the simulation findings.

In 2019, Ahmad et al. [34] for basic and multiple switching instances, SHEPWM was examined for an asymmetrical CHBMLI under unequal DC voltage conditions. By analyzing several switching, additional harmonics might be removed. A sophisticated derivative-free numerical approach handled the problem. Because it eliminated the computation of the Jacobian together its matrix, the approach was simple to use and provided quick computations in each iteration. Also, there was no requirement for an accurate first guess in the vicinity of the real answer because of an identity matrix. To remove the harmonics, distinct inequalities in the dc voltages were used. Only precise switching angle solutions that guaranteed the full removal of specified harmonics were provided. The suggested technology's validity was confirmed by hardware and simulation findings.

In 2020, Barbie et al. [35] have discovered a new analytic phase-voltage weighted THD (WTHD) formula for the voltage of single-phase stair case modulated (SCM) MLI. The formula was a function of entire SA solely, and hence might be simply applied in conventional symbolic/numeric computing tools for SCMMLI of any topology having any count. The WTHD expression produced very reliable data owing to its intellectual character, reducing the danger of round-off and underestimating mistakes linked with traditional frequency-oriented numerical techniques. Moreover, optimal reduction of WTHD was performed out on the basis of the provided method for precise computation of optimal SA, producing minimal WTHD for specified modulation index. A shortened URL was supplied for a downloaded file including MATLAB programmed WTHD routines and the eight look-up tables. Analytical WTHD measurements were compared with outcomes from earlier studies to validate the predicted expression.

In 2017, Baghaee et al. [36] have presented a new ANFIS/Artificial Bee Colony (ABC)-based SHE approach for eliminating the lower order harmonics in MLI with uneven DC sources. The ABC and PSO method are applied for finding the optimal SA of SHE problem. In most instances, ABC was able to identify a fitness function value in the least iteration.

In 2021, Riad et al. [37] have proposed MPA as a method for solving transcendental nonlinear equations in a selective harmonic elimination technique using an MLI. Optimal SA are determined using MPA and they are used to regulate the 11-level CHBMLI. Lower order harmonics are totally eliminated for all modulation indexes from 0 to 1. To determine its efficacy, the constructed algorithm is compared to other existing algorithms.

3. Multilevel Inverter for the Harmonics Elimination

3.1. Multilevel Inverter. One among the most important topologies in the case of MLI series is the cascade MLI [38]. It contains fewer components, a modular construction having a simple switching mechanism, and a count of output voltage levels that may be readily modified by including or deleting cells [39]. The CHBMLI is made up of a series of *H*-bridge, each having itself DC, that may be joined in series to generate output voltage when the right modulation technique is used, as illustrated in Figure 1(a).

$2s + 1$ controls the count of levels, in which s shows the count of *H*-bridges units used. $V_{phn} = Vah_1 + Vah_2$ defines the magnitude, in which Vah_1 and Vah_2 describes the voltages associated to the switching angles of α_1 andα_2, respectively. While other switching mechanisms exist for harmonic reduction and removal [40], the SPWM and SHEPWM were designed to eradicate and remove low-order harmonics, correspondingly.

Figure 1(b) depicts one phase leg of a CHBMLI with 11 levels. Each leg of this configuration requires 20 semiconductor switches and 5 DC sources. The output phase voltage is obtained by summing the voltages generated by all five cells. The output voltage varies from −5 E to 5 E and the waveform is almost a sine wave.

4. Total Harmonic Distortion and SHEPWM Technique in Multiple Inverter

4.1. SHEPWM Technique. The output voltage is stated by equation (1) in this SHEPWM method.

$$g_o(u) = B_0 + \sum_{o=1}^{5} \left(B_o \cos(o\omega u) + W_o \sin(o\omega u)\right). \quad (1)$$

Here, B_0 denotes the DC component of the circuit, i.e.,

$$B_0 = \frac{1}{2\pi} \int_0^{2\pi} g(u). \quad (2)$$

Even harmonics are represented by B_o

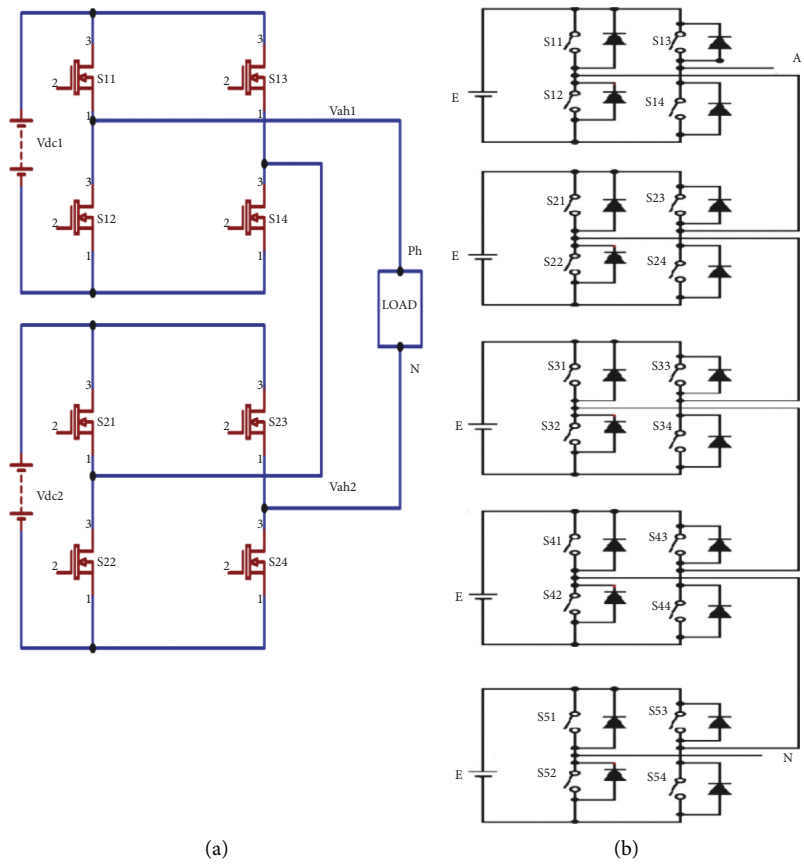

(a) (b)

Figure 1: (a) Five-level single-phase CHBMLI. (b) One phase leg of an 11-level CHBMLI.

$$B_o = \frac{1}{\pi}\int_0^{2\pi} g(u)\sin o\omega u du. \tag{3}$$

Odd harmonics are denoted by the letter W_o

$$W_o = \frac{1}{\pi}\int_0^{2\pi} g(u)\cos o\omega u du. \tag{4}$$

With minimum frequency switching, a more effective output may be obtained. As a result, the output is restricted to $(T-1)$ and the unwanted lower order harmonics are eliminated. The rise in levels count must be done in a specific manner for eradicating the relevant undesirable harmonic content. DC devices, including harmonics, acquire null when the inverter output is 1/4 symmetrical. As a result, equation (1) is reduced to

$$g_o(u) = W_o \sin\left(o\alpha_j\right). \tag{5}$$

When W_o is calculated using

$$W_o = \frac{4W_{dc}}{o\pi}\sum_{j=1}^{t}\left(\left(-R_j\right)^{j+1}\cos\left(o\alpha_j\right)\right), \tag{6}$$

$R_j = (W_{dcj}/W_{dc})$, in which W_{dcj} shows the DC voltage source and W_{dc} shows the ideal DC value

$$W_o = \frac{4W_{dc}}{o\pi}\left[\begin{array}{c} R_1\cos\left(o\alpha_1\right) \pm R_2\cos\left(o\alpha_2\right) \\ \pm R_3\cos\left(o\alpha_3\right) \pm \cdots \pm R_t\cos\left(o\alpha_t\right)\end{array}\right], \tag{7}$$

The "+" sign denotes a rising edge in the above relationship, whereas the "−" sign denotes a declining edge. A stepped waveform is created by combining many switching angles, which may then be divided into degrees of modulation index. Utilizing different modulation indices, the minimising of harmonics leads in the development of minimal frequency switching. Equation (8) contains the basic voltage W_E for the 5th, 7th, 11th, and 13th order harmonics, as well as the modulation index (M) of the constructed 11-level inverter. The dependable switching angles $(\alpha_1, \alpha_2, \alpha_3, \alpha_4, \text{and}\,\alpha_5)$ of the introduced inverter are

achieved employing the SHEPWM approach by utilising equation (9).

$$
\begin{aligned}
W_{fun} &= \frac{4W_{dc}}{\pi}\left[\begin{matrix}\cos(\alpha_1)+\cos(\alpha_2)+\cos(\alpha_3)\\ +\cos(\alpha_4)+\cos(\alpha_5)\end{matrix}\right],\\
W_{5^{th}} &= \frac{4W_{dc}}{5\pi}\left[\begin{matrix}\cos(5\alpha_1)+\cos(5\alpha_2)+\cos(5\alpha_3)\\ +\cos(5\alpha_4)+\cos(5\alpha_5)\end{matrix}\right],\\
W_{7^{th}} &= \frac{4W_{dc}}{7\pi}\left[\begin{matrix}\cos(7\alpha_1)+\cos(7\alpha_2)+\cos(7\alpha_3)\\ +\cos(7\alpha_4)+\cos(7\alpha_5)\end{matrix}\right],\\
W_{11^{th}} &= \frac{4W_{dc}}{11\pi}\left[\begin{matrix}\cos(11\alpha_1)+\cos(11\alpha_2)+\cos(11\alpha_3)\\ +\cos(11\alpha_4)+\cos(11\alpha_5)\end{matrix}\right],\\
W_{13^{th}} &= \frac{4W_{dc}}{13\pi}\left[\begin{matrix}\cos(13\alpha_1)+\cos(13\alpha_2)+\cos(13\alpha_3)\\ +\cos(13\alpha_4)+\cos(13\alpha_5)\end{matrix}\right],\\
M &= \frac{\pi W_E}{4TW_{dc}},
\end{aligned}
\tag{8}
$$

$$
\begin{aligned}
M = \frac{1}{5}&\left[\begin{matrix}\cos(\alpha_1)+\cos(\alpha_2)+\cos(\alpha_2)+\cos(\alpha_3)\\ +\cos(\alpha_4)+\cos(\alpha_5)\end{matrix}\right],\\
&\left[\begin{matrix}\cos(5\alpha_1)+\cos(5\alpha_2)+\cos(5\alpha_2)+\cos(5\alpha_3)\\ +\cos(5\alpha_4)+\cos(5\alpha_5)\end{matrix}\right]=0,\\
&\left[\begin{matrix}\cos(7\alpha_1)+\cos(7\alpha_2)+\cos(7\alpha_2)+\cos(7\alpha_3)\\ +\cos(7\alpha_4)+\cos(7\alpha_5)\end{matrix}\right]=0,\\
&\left[\begin{matrix}\cos(11\alpha_1)+\cos(11\alpha_2)+\cos(11\alpha_2)+\cos(11\alpha_3)\\ +\cos(11\alpha_4)+\cos(11\alpha_5)\end{matrix}\right]=0,\\
&\left[\begin{matrix}\cos(13\alpha_1)+\cos(13\alpha_2)+\cos(13\alpha_2)+\cos(13\alpha_3)\\ +\cos(13\alpha_4)+\cos(13\alpha_5)\end{matrix}\right]=0.
\end{aligned}
\tag{9}
$$

Equation (8) may be used to compute the appropriate firing angles, which must meet the following relationships:

$$0 \le \alpha_1 \le \alpha_2 \le \alpha_3 \le \alpha_4 \le \alpha_5 \le \frac{\pi}{2}. \tag{10}$$

The suggested MLI operates at the basic frequency having five sources, resulting in a total of $2^5 = 32$ distinct switching patterns. Only 9 of these designs have rectified waveforms, whereas 16 are mirror images of the horizontal axis. The only one-quarter waveform and the comparable waveform incorporating symmetries are due to symmetry. Due to the obvious nonlinear transcendental character of the SHEPWM equations, the solution is difficult. As a result, the generated solutions may be used to delete the specified harmonic content.

4.2. THD. THD is the sum of all harmonic components of a voltage or current waveform compared to the fundamental component of the voltage or current waveform.

It will be explained how to measure the THD of line voltage using the suggested approach in light of including the waveform. The following equation can be used to calculate THD.

$$\text{THD} = \sqrt{\frac{2}{3}\left(\frac{w_{rms}^2}{w_1^2}\right) - 1}. \tag{11}$$

Factor 2 is multiplied to transform the amplitude of W_1 to the RMS ofW_1, and element 3 is multiplied to transform the amplitude of phase voltage to the amplitude of line voltage.

$$W_{rms} = \sqrt{\frac{1}{2\pi}\int_0^{2\pi} w^2(\alpha)\mathrm{d}\alpha}. \tag{12}$$

A technique for calculating the W_{rms} of line voltage is shown here. Since the phase voltages are given at the angles, the W_{rms} associated with the phase voltage may be easily determined. However, it reveals the issue with calculating the W_{rms} of line voltage. The line voltage (W_{bc}) has been obtained physically by deducting phase voltage W_c fromW_b, which is recognized with MLI with distinct dc sources by two separate angle groups. The development process, which is described by equation (13) as a component of the switching edge (α), may be used to illustrate this staircase voltage.

$$V(\alpha - \alpha_j) = \begin{cases} 1, & \alpha > \alpha_j,\\ 0, & \alpha < \alpha_j. \end{cases} \tag{13}$$

A functional structure voltage's half-cycle waveform is described by

$$
\begin{aligned}
q(\alpha) = {}& [W_{dc1}V(\alpha-\alpha_1)] + \cdots [W_{dct}V(\alpha-\alpha_1)]\\
&- [W_{dct}V(\alpha-(\pi-\alpha_t))] + \cdots [W_{dc1}V(\alpha-(\pi-\alpha_t))].
\end{aligned}
\tag{14}
$$

In this symmetric waveform, the condition of the second half-wave is identical to $q(\alpha)$, but it is positioned just beneath the horizontal axis. As a result, the phase voltage is increased.

$$W_b(\alpha) = q(\alpha) - q(\alpha - \pi). \tag{15}$$

Performing a $2\pi/3$-rad phase move to the voltage of a phase yields W_c. $W_b(\alpha)$ is represented by the interval $(0 - 2\pi)$; similarly, W_c is defined by the following equation:

$$W_c(\alpha) = \begin{cases} W_\alpha\left(\alpha + \dfrac{2\pi}{3}\right), & 0 < \alpha < \dfrac{4\pi}{3},\\[2ex] W_\alpha\left(\alpha - \dfrac{2\pi}{3}\right), & 0 > \alpha > \dfrac{4\pi}{3}. \end{cases} \tag{16}$$

Finally, deducting $W_c(\alpha)$ from $W_b(\alpha)$ yields the line voltage required for advancement work. W_{bc} contains a constant inducement in each of the two adjacent places $(\alpha l, \alpha l + 1)$. The total of these results solves the basic, and W_{rms} and THD are determined as a result.

5. Enhanced Recurrent Neural Network and Multi-Group Marine Predator Algorithm for the Multilevel Inverter

5.1. Enhanced RNN. An RNN is a form of artificial neural network that works with time series or sequential data. It is the first algorithm with an internal memory that remembers its input, making it ideal for machine learning problems involving sequential data. It is one of the algorithms responsible for the incredible advances in deep learning over the last few years. These are derived from feedforward networks, behave similarly to human brains.

There are several different types of RNNs. It introduces multiple gates to open and block entry to the error flow, as well as a memory cell that permits "constant error carrousels" [41]. The peephole long short-term memory (LSTM) is another LSTM version that describes the gates to see the cell state. Gated recurrent units (GRU) describe a simplified version of LSTM. The main distinction between GRU and LSTM is that GRU's bag has two gates: reset and update, but LSTM's bag has three gates: input, output, and forget. Because GRU has fewer gates than LSTM, it is less complicated. If the dataset is tiny, GRU should be used; otherwise, LSTM should be used for larger datasets. The memory and fresh input information are controlled by a reset gate as well as an update gate in a GRU. When LSTM and GRU are compared, there exists no obvious victor which varies depending on the application job [42]. In LSTM, a divergent gating strategy is developed that uses the gradient of the cell state to regulate the flow and has been shown to be successful for action recognition. Another successful solution to the vanishing gradient issue is residual connection.

The output response i_u at time step u is derived as below from the input y_u and the output i_{u-1} of the previous time slot for a conventional RNN layer:

$$i_u = \tanh\left(X_{yi} y_u + X_{ii} i_{u-1} + c_i\right). \tag{17}$$

Here, $X_{\alpha\beta}$ indicates the weight matrix associated with α and β, and $\alpha \in \{y, i\}$, $\beta \in \{i\}$, and c_γ represent the bias vector, while$\gamma \in \{i\}$.

The RNN offers advantages like better time series prediction, extends efficient pixel neighbourhood, etc. but, it limits from exploding gradient or vanishing problem, difficult training procedures, etc. Hence, to overcome the limitations, the hidden neurons of RNN are tuned by MGMPA with the intention of HDP minimization thus known as ERNN. This ERNN solves the gradient descent problem and also saves the training time.

5.2. Objective Function. The goal is to alter the basic output voltage element while keeping the HDP as low as possible. The suggested method is implemented by resolving a bi-objective function for the group of PSAs $(\alpha = \{\alpha_1, \alpha_2, \ldots, \alpha_N\})$, which act as the model parameters, identical to existing HDP minimizations. A common definition of such a fitness function is as follows:

$$\text{fit}_{ob}(\alpha) = \text{fit}_{\text{ME}}(\alpha) + \text{fit}_{HDP}(\alpha), \tag{18}$$

$\text{fit}_{\text{ME}}(\alpha)$ is the modulation error (ME) expression described in (19) and $\text{fit}_{HDP}(\alpha)$ shows the HDP expression. Irrespective of the goal MI value, both the ME and HDP statements are given equal weight.

$$\text{fit}_{\text{ME}}(\alpha) = \varepsilon_n = 100 \cdot \left|\frac{n_b - n_U}{n_U}\right|. \tag{19}$$

Equation (19) defines the % ME expression, in which n_b shows the actual MI and n_U defines the intended (reference) MI value $(0 \le n_U \le 1.1)$.

5.3. MGMPA Algorithm. The MPA describes an optimization algorithm based on predator and prey behavior while catching their own food. MPA is straightforward and easier to apply. It performs well in optimization issues. However, due to an imbalance in its exploration and exploitation skills, it converges prematurely. This research presents an MGMPA [43] to increase the performance of MPA. The multigroup mechanism divides the original population into a number of distinct groups. After a given repetition, these groups produce the Elite matrix and top predator using various tactics and communicate information. The maximum of the identical group, the average of the identical group, the maximum of various groups, and the average of various groups are among the tactics mentioned above.

The multigroup process divides the original population into numerous groups that are each individually optimised. After a set repetition, these groups create the top predator using various tactics. The suggested MGMPA may accomplish collaborative work across groups and improve the usage of every solution by using a multigroup mechanism and producing approaches.

5.3.1. Generation Strategies. To discover food, the top predator constructs an Elite matrix as part of the optimization procedure. As a result, the top predator is crucial to the algorithm's optimization procedure. The portion will suggest four producing ways to produce the Elite matrix and top predator, in order to enhance MMA performance even more.

(1) Generation Strategy. The optimal answer of a group of people. If the parameters associated with the solutions are autonomous during the optimization procedure, it is simpler to produce better outcomes by just exchanging knowledge inside the similar group. As a result, when itr = oS iteration $(o = 1, 2, 3 \ldots)$, the best solution $y_{\text{best},h}(u)$ of the identical group creates an Elite matrix in method 1.

$$y_{\text{best},h}(u) = \text{Best}\left\{y_{1,h}(u), y_{2,h}(u), \ldots, y_{o,h}(u)\right\}. \tag{20}$$

Here, $y_{1,h}(u), y_{2,h}(u), \ldots, y_{o,h}(u)$ denote the h^{th} group's o solutions.

(2) Generation Strategy 2. The average of the identical group's solutions. The impact of strategy 2 is the same as that of strategy 1. In method 2, where itr = oS iteration $(o = 1, 2, 3 \ldots)$, the average solution $y_{\text{avg},h}(u)$ is produced by averaging the l good methods of the similar group for population diversity. To make an Elite matrix, utilize $y_{\text{avg},h}(u)$.

$$y_{\text{avg},h}(u) = \frac{y_{1,h}(u), y_{2,h}(u), \ldots, y_{o,h}(u)}{l}. \tag{21}$$

The l proper result of the h^{th} group is represented by $y_{1,h}(u), y_{2,h}(u), \ldots, y_{o,h}(u)$.

(3) Generation Strategy 3. The entire groups' optimal method. If the parameters linked with the solutions are weakly associated during the optimization procedure, it is simpler to lead to better outcomes by exchanging information across all groups. As a result, when itr = oS iteration $(o = 1, 2, 3 \ldots)$ is employed in strategy 3, the optimal option $y_{\max}(u)$ of the entire groups is utilised to generate an Elite matrix.

$$y_{\max}(u) = \text{Best}\{y_1(u), y_2(u), \ldots, y_O(u)\}, \tag{22}$$

O Solutions in the complete groups are represented by $y_1(u), y_2(u), \cdots, y_O(u)$.

(4) Generation Strategy 4. The average of the entire groups' solutions. The impact of strategy 4 is the identical as that of Strategy 3. In method 4, when itr = oS iteration $(o = 1, 2, 3 \ldots)$, the average solution $y_{\text{avg}}(u)$ is computed by summing the optimal answer of every group for population diversity. To make an Elite matrix, employ $y_{\text{avg}}(u)$.

$$y_{\text{avg}}(u) = \frac{y_{\max,1}(u), y_{\max,2}(u), y_{\max,3}(u), \ldots, y_{\max,H}(u)}{H}. \tag{23}$$

The optimal solution of every group is represented by $y_{\max,1}(u), y_{\max,2}(u), y_{\max,3}(u), \ldots, y_{\max,H}(u)$. The letter H stands for the count of groups.

5.4. MGMPA Implementation Process. This study suggests the MGMPA implementation procedure based on the four generating strategies mentioned above. The planned MGMPA includes four groups in the process. To run autonomously, the four groups will use distinct techniques. After a certain number of iterations, every group will use various techniques to reach the top predator and Elite matrix. Consequently, the global optimal solution is determined by the best solution of the entire groups. The pseudo code of introduced MGMPA is depicted in Algorithm 1 and its flowchart is in Figure 2.

Algorithm 1. Introduced MGMPA.

Start

Population initialization

Parameter initialization

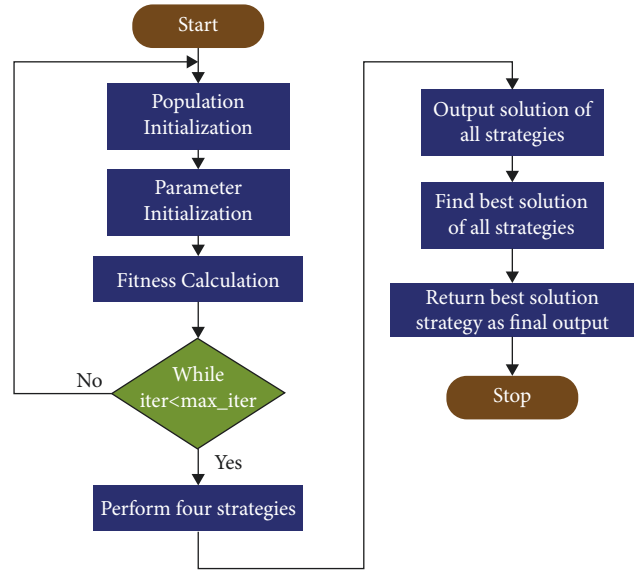

Figure 2: Flowchart of MGMPA.

Fitness calculation

While itr ≤ max_itr

Perform strategy 1

$$y_{\text{best},h}(u) = Best\{_{1,h}(u), y_{2,h}(u), \ldots, y_{o,h}(u)\}. \tag{24}$$

Perform strategy 2

$$y_{\text{avg},h}(u) = \frac{y_{1,h}(u), y_{2,h}(u), \ldots, y_{o,h}(u)}{l}. \tag{25}$$

Perform strategy 3

$$y_{\max}(u) = \text{Best}\{y_1(u), y_2(u), \ldots, y_O(u)\}. \tag{26}$$

Perform strategy 4

$$y_{avg}(u) = \frac{y_{\max,1}(u), y_{\max,2}(u), y_{\max,3}(u), \ldots, y_{\max,H}(u)}{H}. \tag{27}$$

Output solution of all strategies

Find the best solution of all strategies

The strategy with best solution is returned as final output

Stop.

6. Results and Discussion

6.1. Experimental Setup. The proposed MGMPA-THD was compared with various heuristic-based algorithms such as Harris Hawks optimization (HHO)-THD [44], Whale optimization algorithm (WOA)-THD [45], and MPA-THD [46] in terms of several analysis such as THD analysis, voltage analysis, convergence analysis, and HDP analysis to describe the superiority of the recommended method. This method is highly recommended for both reduced as well as traditional component types MLIs. The harmonics can easily

be eliminated by any form of optimization algorithms with the deep learning methods.

6.2. THD Analysis. The suggested MGMPA-THD approach gives the lowest current-THD among the three known optimization methods when the load's neutral is not linked to the MLI's points, as shown in Figure 3 and Table 1. The outcomes are measured in terms of modulation index against current THD. At a modulation index of 0.7, the MGMPA-THD is 3%, 3.5%, and 4% superior to MPA-THD, HHO-THD, and WOA-THD, respectively. Hence, it can be confirmed that MGMPA-THD is better than the other methods for the introduced MLI model.

6.3. Voltage Analysis. The line-voltage waveform of a suggested system was shown in Figure 4. The waveform contains eleven levels, as can be seen. As a result, determining its RMS value is more difficult than computing the phase voltage, and obtaining a single mathematical equation for the RMS value associated with the whole range of SAs is difficult. The input signal voltage ranges from 0 to 0.8 volts in the case of a low logic state and 2 to 5 volts in the case of a high logic state. Similarly, the minimum output high voltage is 2.7 V.

6.4. Convergence Analysis. Table 2 shows the relationship among cost function and modulation lists. It can be seen that the cost function in MGMPA-THD is better at $m = 1$ with a cost function of 2.80 percent. In Figure 5, the suggested MGMPA-THD connection maintains the reduced distortion (0.5–1.0) for the modulation period (0.9–1.0) in the output above the existing methods. In this approach, the suggested technology improves the output waveform by reducing convergence. The recommended MGMPA-THD approach has been examined using numerous factors since the most fundamental evaluation and has made correctness come true when compared to certain other old techniques.

6.5. Harmonic Distortion Parameter Analysis. The study of this distortion is unique. A single-frequency sinusoidal signal is applied to the circuit, and the output is monitored and examined with distortion.

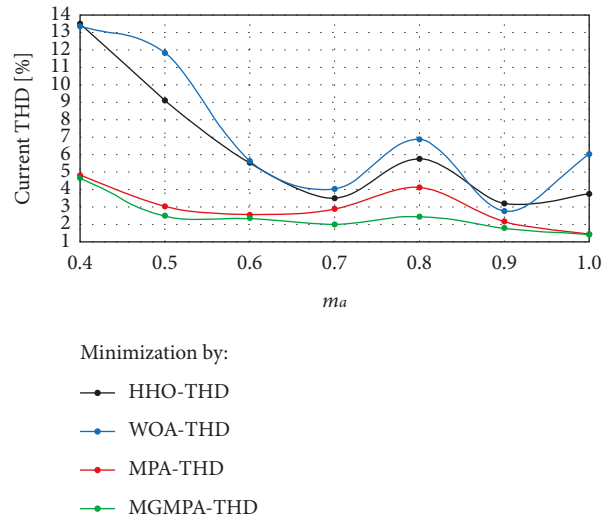

Figure 3: THD analysis of various optimization algorithms.

When the input signal is supplied to the circuit, distortion in the output signal may occur due to the nonlinear characteristics of the components. As a result, the reference signal may appear at multiple frequency positions in the output. THD, THD plus noise (THDN), signal to noise and distortion (SINAD), signal-to-noise ratio (SNR), and nth harmonic value with respect to the fundamental frequency can also be determined using this harmonic distortion measuring approach.

THD quantifies the unwanted harmonics that are prevailed in the voltage or current waveforms whereas HDP are common voltage and current variations that are caused mainly due to changes in frequencies.

Figure 6 shows the voltage of an 11-level CHBMLI generated employing the MGMPA-THD and different approaches at minimal THD. At a frequency of 50 Hz, the matching fundamental line voltage was generated. The graph shows the HDP analysis at various modulation indexes. It can be seen that the parameter distortion is achieved less with MGMPA-THD than the existing methods in majority of the modulation indices. Therefore, it can be revealed that the suggested MGMPA-THD is better than the other methods in terms of HDP analysis.

Table 1: THD analysis of different optimization algorithms.

Methods	Modulation index						
	$m_a = 0.4$	$m_a = 0.5$	$m_a = 0.6$	$m_a = 0.7$	$m_a = 0.8$	$m_a = 0.9$	$m_a = 1.0$
HHO-THD [44]	13.5	9	5.5	3.5	5.8	3.2	3.8
WOA-THD [45]	13.3	12	5.6	4	7	2.9	6
MPA-THD [46]	5	3	2.5	3	4	2.2	1.6
MGMPA-THD	4.5	2.5	2.2	2	2.5	1.9	1.5

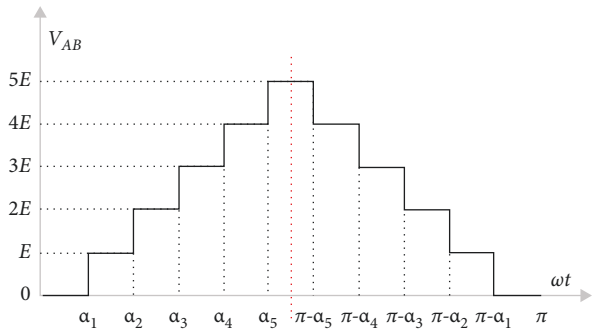

Figure 4: Line-to-line voltage of introduced MLI.

Table 2: Convergence analysis of various optimization algorithms.

Modulation index	0.4	0.6	0.8	1
HHO-THD [44]	37.21	24.33	15.54	6.96
WOA-THD [45]	35.56	20.34	12.78	3.02
MPA-THD [46]	36.01	21.23	13.12	5.06
MGMPA-THD	30.31	18.34	10.14	2.80

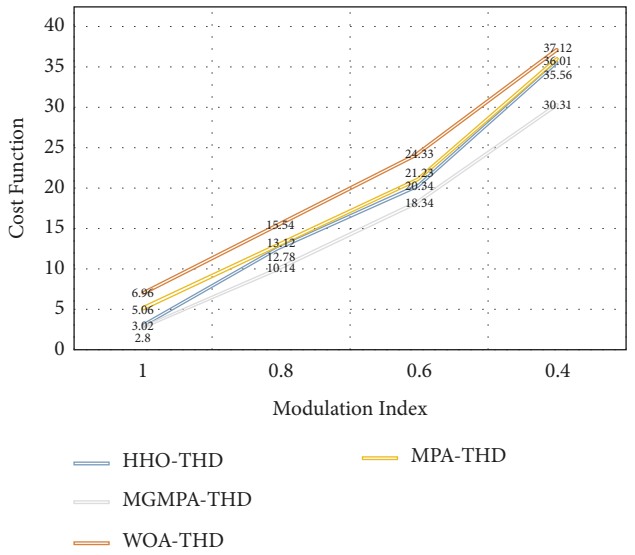

Figure 5: Convergence analysis of various optimization algorithms.

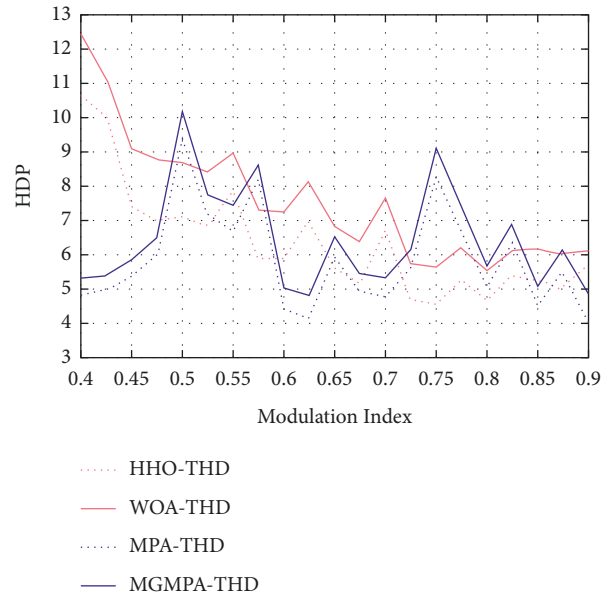

Figure 6: HDP analysis of various optimization algorithms.

7. Conclusion

This study introduced the MGMPA for solving transcendental nonlinear equations with an MLI in a SHE method. Its relevance and superiority over current research-based SHE techniques might be due to its high accuracy, high chance of convergence, and better output voltage quality. The optimum SAs from MPA were used to manage a three-phase 11-level MLI employing CHB architecture to regulate the critical element and remove the harmonics for complete values of modulation index. The downside of SHE is that it is difficult to solve nonlinear problems with it. As a result, specialised optimization techniques are required. AI algorithms could effectively solve such a nonlinear transcendental equation; however, their time consumption and convergence abilities differ. The ERNN is an RNN in which the hidden neurons were modified by MGMPA with the goal of minimize HDP. Simulation and analytical results confirmed the method's resiliency and consistency. According to simulation data, the MGMPA approach was more effective and suitable than numerous algorithms such as the MPA, HHO, and WOA.

Symbols

s:	Count of H bridges
α:	Switching angle
V_{ah1}:	Voltage associated to the switching angle α_1
V_{ah2}:	Voltage associated to the switching angle α_2
V_{phn}:	Output voltage magnitude
u:	Time step
o:	Iteration count
ω:	Angular frequency
g_o (u):	Output voltage
B_0:	DC component of the circuit
B_o:	Even harmonics
W_o:	Odd harmonics
T:	Time period
α_j:	Dependable switching angles
W_{dcj}:	DC voltage source
W_{dc}:	Ideal DC value
W_{dct}:	Discrete cosine transform voltage
W_1:	Voltage of first half-wave
W_{dc1}:	DC voltage of first half-wave
W_E:	Basic voltage
M:	Modulation index
W_{rms}:	RMS voltage
W_{bc}:	Line voltage
W_b, W_c:	Phase voltages
$V(\alpha-\alpha_j)$:	Staircase voltage
$q(\alpha)$:	Functional structure voltage's half cycle waveform
$W_b(\alpha)$, $W_c(\alpha)$:	Phase voltage at the respective switching angle
i_u:	Input gate
X_{yi}, y_{ii}:	Weight matrices
y_u:	Input at unit step
$X_{\alpha\beta}$:	Weight matrix associated with α and β, and $\alpha \in \{y, i\}$, $\beta \in \{i\}$
c_γ:	Bias vector, while $\gamma \in \{i\}$
i_{u-1}:	Output of the previous time slot
$\text{fit}_{ob}(\alpha)$:	Fitness function
$\text{fit}_{ME}(\alpha)$:	Modulation error
$\text{fit}_{HDP}(\alpha)$:	HDP expression
n_b:	Actual MI
n_U:	Intended (reference) MI value
itr:	Iteration
$y_{best,h}(u)$:	Best solution
$y_{avg,h}(u)$:	Average of the identical group's solutions
l:	Result of the h^{th} group
$y_{1,h}(u), y_{2,h}(u), \ldots, y_{0,h}(u)$:	h^{th} group's o solutions
$y_{max}(u)$:	Optimal option
$y_{avg}(u)$:	Average of the entire group's solutions
H:	Count of groups.

Data Availability

The reference articles data used to support the findings of this study are included within this article.

Disclosure

The authors received no specific grant from any funding agency in the public, commercial, or not-for-profit sectors.

Conflicts of Interest

The authors declare that they have no conflicts of interest.

References

[1] P. Omer, J. Kumar, B. S. Surjan, and B. S. Surjan, "A review on reduced switch count multilevel inverter topologies," *IEEE Access*, vol. 8, pp. 22281–22302, 2020.

[2] A. K. Yadav, K. Gopakumar, K. Raj, L. Umanand, S. Bhattacharya, and W. Jarzyna, "A hybrid 7-level inverter using low-voltage devices and operation with single DC-link," *IEEE Transactions on Power Electronics*, vol. 34, no. 10, pp. 9844–9853, 2019.

[3] F. Wang, "Sine-triangle versus space-vector modulation for three-level PWM voltage-source inverters," *IEEE Transactions on Industry Applications*, vol. 38, no. 2, pp. 500–506, 2002.

[4] H. S. Patel and R. G. Hoft, "Generalized techniques of harmonic elimination and voltage control in thyristor inverters: part I-harmonic elimination," *IEEE Transactions on Industry Applications*, vol. IA-9, no. 3, pp. 310–317, 1973.

[5] G. Chitrakala, N. Stalin, and V. Mohan, "A segmented ladder structured multilevel inverter for switch count remission and dual-mode savvy," *Journal of Circuits, Systems, and Computers*, vol. 27, no. 14, Article ID 1850223, 2018.

[6] S. Ahmad, A. Iqbal, and M.-H. I. Ashraf, "Selected harmonics elimination in multilevel inverter using improved numerical technique," in *Proceedings of the 2018 IEEE 12th International Conference on Compatibility, Power Electronics and Power Engineering (CPE-POWERENG 2018)*, Doha, Qatar, April 2018.

[7] M. D. Siddique, S. Mekhilef, N. M. Shah et al., "Low switching frequency based asymmetrical multi level inverter topology with reduced switch count," *IEEE Access*, vol. 7, pp. 86374–86383, 2019.

[8] V. Mohan, N. Stalin, and S. Jeevananthan, "A tactical chaos based PWM technique for distortion restraint and power spectrum shaping in induction motor drives," *International Journal of Power Electronics and Drive Systems*, vol. 5, no. 3, p. 383, 2015.

[9] S. Kundu, S. Bhowmick, and S. Banerjee, "Improvement of power utilisation capability for a three-phase seven-level CHB inverter using an improved selective harmonic elimination–PWM scheme by sharing a desired proportion of power among the H-bridge cells," *IET Power Electronics*, vol. 12, no. 12, pp. 3242–3253, 2019.

[10] M. Al-Hitmi, S. Ahmad, A. Iqbal, S. Padmanaban, and I. Ashraf, "Selective harmonic elimination in a wide modulation range using modified newton–raphson and pattern

generation methods for a multilevel inverter," *Energies*, vol. 11, no. 2, p. 458, 2018.

[11] K. Sundareswaran, K. Jayant, and T. N. Shanavas, "Inverter harmonic elimination through a colony of continuously exploring ants," *IEEE Transactions on Industrial Electronics*, vol. 54, no. 5, pp. 2558–2565, 2007.

[12] V. Mohan, J. Raja, and S. Jeevananthan, "A random PWM scheme based on coalescing the pseudorandom triangular carrier and the randomized pulse position for voltage source inverters," *CiiT International Journal of Programmable Device Circuits and Systems*, vol. 4, no. 11, pp. 570–574, 2012.

[13] K. Ganesan, K. Barathi, P. Chandrasekar, and D. Balaji, "Selective harmonic elimination of cascaded multilevel inverter using BAT algorithm," *Procedia Technology*, vol. 21, pp. 651–657, 2015.

[14] V. Mohan, G. Chitrakala, and N. Stalin, "A low frequency PWM based multilevel DC-link inverter with cascaded sources," *Asian Journal of Research in Social Sciences and Humanities*, vol. 7, no. 1, p. 686, 2017.

[15] T. Sudhakar Babu, K. Priya, D. Maheswaran, K. Sathish Kumar, and N. Rajasekar, "Selective voltage harmonic elimination in PWM inverter using bacterial foraging algorithm," *Swarm and Evolutionary Computation*, vol. 20, pp. 74–81, 2015.

[16] V. Mohan and S. Senthilkumar, "IoT based fault identification in solar photovoltaic systems using an extreme learning machine technique," *Journal of Intelligent and Fuzzy Systems*, In press, 2022.

[17] R. Sitharthan, M. Karthikeyan, D. S. Sundar, and S. Rajasekaran, "Adaptive hybrid intelligent MPPT controller to approximate effectual wind speed and optimal rotor speed of variable speed wind turbine," *ISA Transactions*, vol. 96, pp. 479–489, 2020.

[18] M. A. Memon, M. D. Siddique, M. Saad, and M. Mubin, "Asynchronous particle swarm optimization-genetic algorithm (APSO-GA) based selective harmonic elimination in a cascaded H-bridge multilevel inverter," *IEEE Transactions on Industrial Electronics*, vol. 25, 2021.

[19] S. Senthilkumar, V. Mohan, S. P. Mangaiyarkarasi, and M. Karthikeyan, "Analysis of single-diode PV model and optimized MPPT model for different environmental conditions," *International Transactions on Electrical Energy Systems*, vol. 2022, Article ID 4980843, 17 pages, 2022.

[20] C. Bharatiraja, S. Jeevananthan, R. Latha, and V. Mohan, "Vector selection approach-based hexagonal hysteresis space vector current controller for a three phase diode clamped MLI with capacitor voltage balancing," *IET Power Electronics*, vol. 9, no. 7, pp. 1350–1361, 2016.

[21] F. Filho, L. M. Tolbert, Y. Cao, and B. Ozpineci, "Real-time selective harmonic minimization for multilevel inverters connected to solar panels using artificial neural network angle generation," *IEEE Transactions on Industry Applications*, vol. 47, no. 5, pp. 2117–2124, 2011.

[22] M. Balasubramonian and V. Rajamani, "Design and real-time implementation of SHEPWM in single-phase inverter using generalized hopfield neural network," *IEEE Transactions on Industrial Electronics*, vol. 61, no. 11, pp. 6327–6336, 2014.

[23] F. Glover, "Future paths for integer programming and links to artificial intelligence," *Computers and Operations Research*, vol. 13, no. 5, pp. 533–549, 1986.

[24] M. Ali, M. Tariq, K. A. Lodi et al., "Robust ANN-based control of modified PUC-5 inverter for solar PV applications," *IEEE Transactions on Industry Applications*, vol. 57, no. 4, pp. 3863–3876, 2021.

[25] A. Moeed Amjad and Z. Salam, "A review of soft computing methods for harmonics elimination PWM for inverters in renewable energy conversion systems," *Renewable and Sustainable Energy Reviews*, vol. 33, pp. 141–153, 2014.

[26] S. Ahmad, A. Iqbal, M. Ali, K. Rahman, and A. S. Ahmed, "A fast convergent homotopy perturbation method for solving selective harmonics elimination PWM problem in multi level inverter," *IEEE Access*, vol. 9, pp. 113040–113051, 2021.

[27] S.-M. Kim and K.-B. Lee, "A modified third harmonic pulse-width modulation for reduced switching loss in cascaded H-bridge multilevel inverters," *IFAC-PapersOnLine*, vol. 52, no. 4, pp. 472–476, 2019.

[28] E. Barbie, R. Rabinovici, and A. Kuperman, "Analytical formulation and optimization of weighted total harmonic distortion in three-phase staircase modulated multilevel inverters," *Energy*, vol. 215, Article ID 119137, 2021.

[29] C. Buccella, M. G. Cimoroni, and C. Cecati, "Mathematical proof of a harmonic elimination procedure for multilevel inverters," *Mathematics and Computers in Simulation*, vol. 184, pp. 69–81, 2021.

[30] R. Gunasekaran and C. Karthikeyan, "Nonlinear transformational optimization (NTO) technique based total harmonics distortion (THD) reduction of line to line voltage for multi-level inverters," *Microprocessors and Microsystems*, vol. 74, Article ID 102998, 2020.

[31] G. N. Rao, P. Sangameswara Raju, and K. Chandra Sekhar, "Harmonic elimination of cascaded H-bridge multilevel inverter based active power filter controlled by intelligent techniques," *International Journal of Electrical Power and Energy Systems*, vol. 61, pp. 56–63, 2014.

[32] T. R. Sumithira and A. Nirmal Kumar, "Elimination of harmonics in multilevel inverters connected to solar photovoltaic systems using ANFIS: an experimental case study," *Journal of Applied Research and Technology*, vol. 11, no. 1, pp. 124–132, 2013.

[33] S. Sudha Letha, T. Thakur, and J. Kumar, "Harmonic elimination of a photo-voltaic based cascaded H-bridge multilevel inverter using PSO (particle swarm optimization) for induction motor drive," *Energy*, vol. 107, pp. 335–346, 2016.

[34] S. Ahmad, M. Meraj, A. Iqbal, and I. Ashraf, "Selective harmonics elimination in multilevel inverter by a derivative-free iterative method under varying voltage condition," *ISA Transactions*, vol. 92, pp. 241–256, 2019.

[35] E. Barbie, R. Rabinovici, and A. Kuperman, "Analytic formulation and optimization of weighted total harmonic distortion in single-phase staircase modulated multilevel inverters," *Energy*, vol. 199, Article ID 117470, 2020.

[36] H. R. Baghaee, M. Mirsalim, G. B. Gharehpetian, H. A. Talebi, and A. Niknam-Kumle, "A decentralized power management and sliding mode control strategy for hybrid AC/DC microgrids including renewable energy resources," *IEEE Transactions on Industrial Informatics*, vol. 99, p. 1, 2017.

[37] N. Riad, W. Anis, A. Elkassas, and A. E.-W. Hassan, "Three-phase multilevel inverter using selective harmonic elimination with marine predator algorithm," *Electronics*, vol. 10, no. 4, p. 374, 2021.

[38] G. Chitrakala, N. Stalin, and V. Mohan, "Normally bypassed cascaded sources multilevel inverter with RGA optimization for reduced output distortion and formulaic passive filter design," *Journal of Circuits, Systems, and Computers*, vol. 29, no. 2, Article ID 2050019, 2019.

[39] J. Rodriguez, J. S. Lai, and F. Z. Peng, "Multilevel inverters: a survey of topologies, controls, and applications," *IEEE*

Transactions on Industrial Electronics, vol. 49, no. 4, pp. 724–738, 2002.

[40] S. Kouro, M. Malinowski, K. GopaKumar et al., "Recent advances and industrial applications of multilevel converters," *IEEE Transactions on Industrial Electronics*, vol. 57, no. 8, pp. 2553–2580, 2010.

[41] R. Sitharthan and M. Geethanjali, "An adaptive elman neural network with C-PSO learning algorithm based pitch angle controller for DFIG based WECS," *Journal of Vibration and Control*, vol. 23, no. 5, pp. 716–730, 2017.

[42] P. Zhang, J. Xue, C. Lan, W. Zeng, Z. Gao, and N. Zheng, "EleAtt-RNN: adding attentiveness to neurons in recurrent neural networks," *IEEE Transactions on Image Processing*, vol. 29, pp. 1061–1073, 2020.

[43] J.-S. Pan, J. Shan, J. Shan, S.-J. Jiang, S.-J. Jiang, and L. Liao, "A multigroup marine predator algorithm and its application for the power system economic load dispatch," *Energy Science and Engineering*, vol. 2021, pp. 1–15, 2021.

[44] A. A. Heidari, S. Mirjalili, I. Aljarah, M. Mafarja, M. Mafarja, and H. Chen, "Harris hawks optimization: algorithm and applications," *Future Generation Computer Systems*, vol. 97, pp. 849–872, 2019.

[45] A. Alizada, "The whale optimization algorithm," *Advances in Engineering Software*, vol. 95, 2021.

[46] A. Faramarzi, M. Heidarinejad, S. Mirjalili, and A. H. Gandomi, "Marine predators algorithm: a nature-inspired metaheuristic," *Expert Systems with Applications*, vol. 152, 2020.